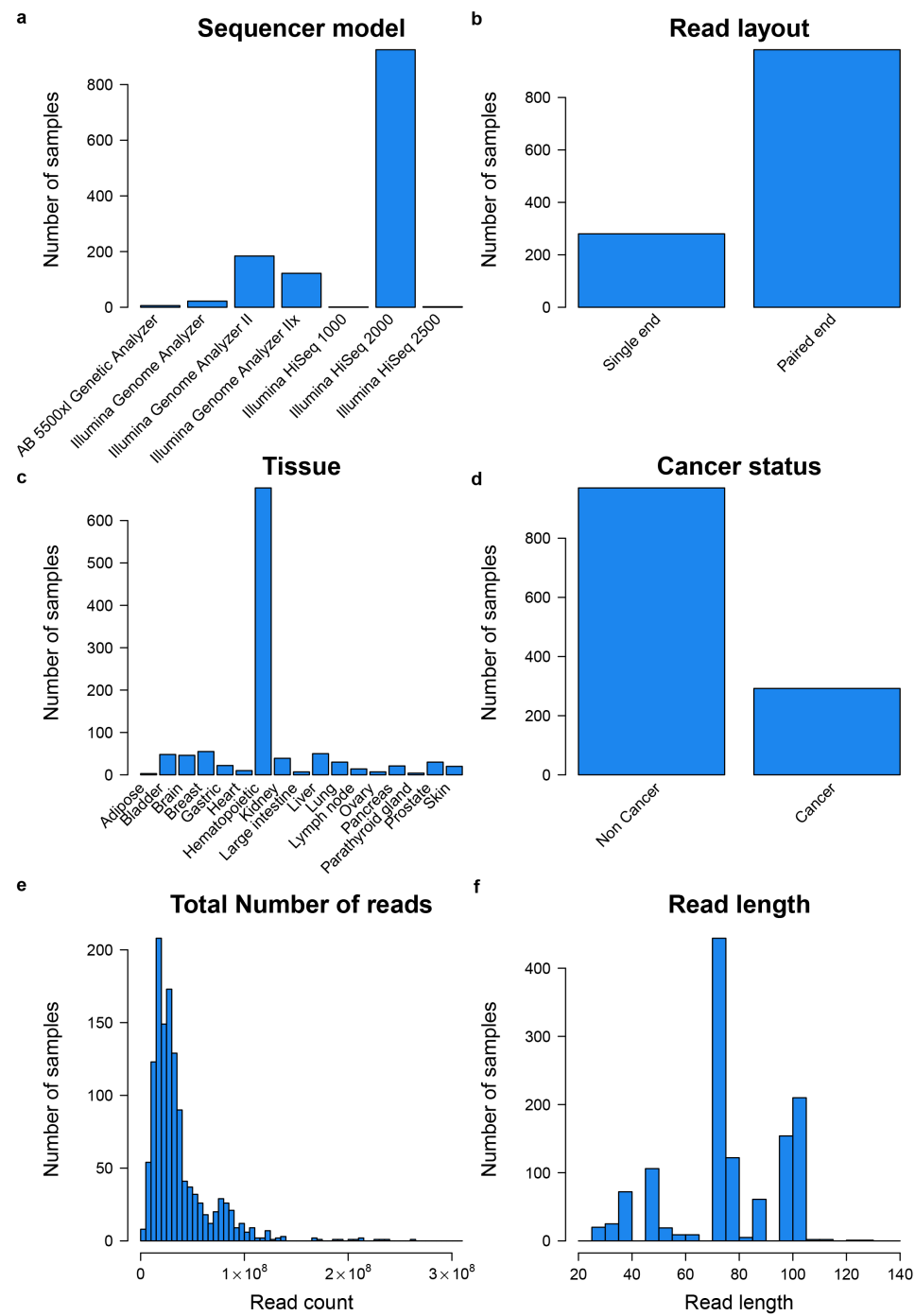


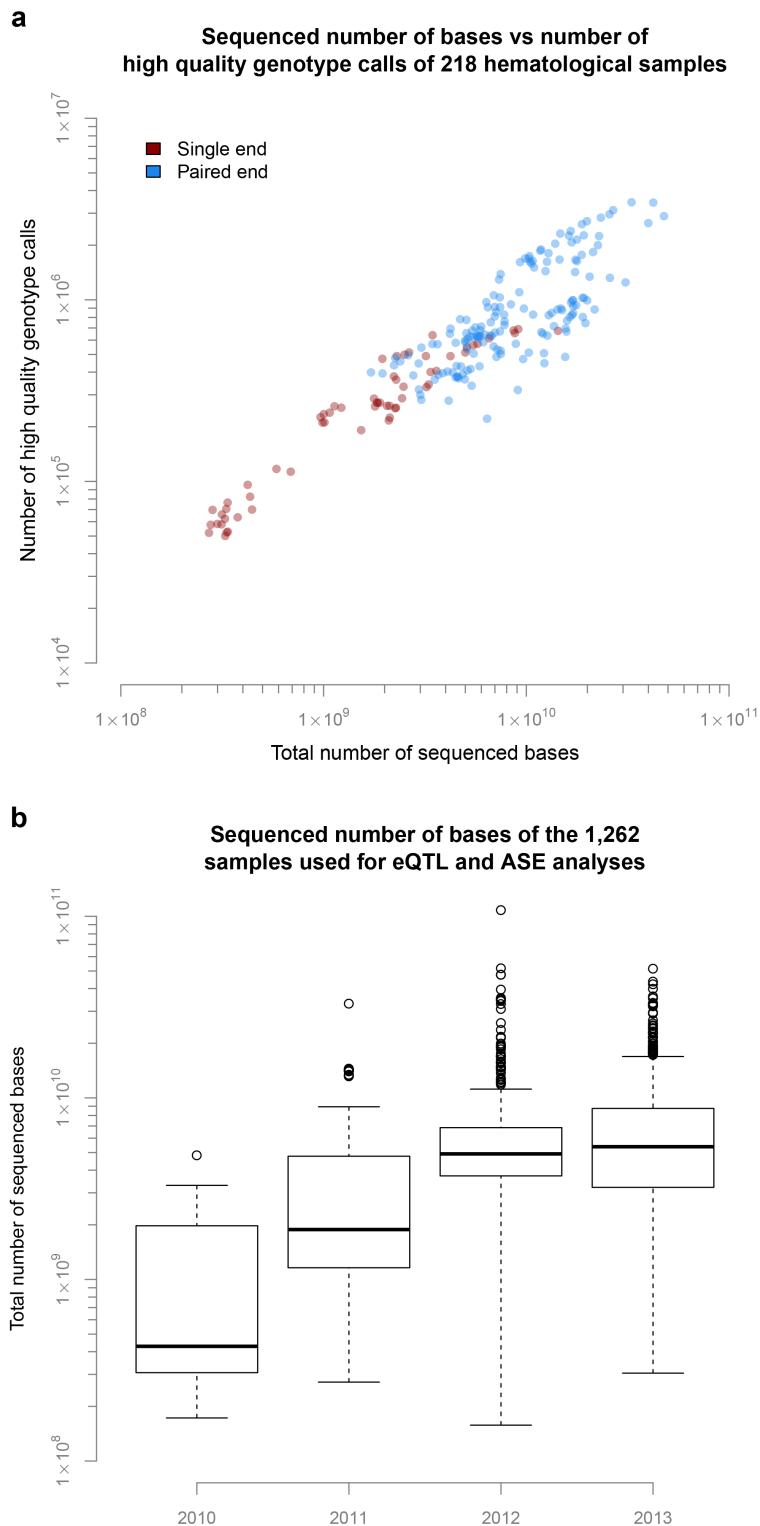
Supplementary Figure 1



Overview of the properties of the 1,262 samples used for eQTL and ASE analyses.

Here we show that the samples which we successfully genotyped and used for the eQTL and ASE analysis still show high heterogeneity in sequencer models (a), read layout (b), sampled tissue (c), cancer status (d), total number of reads (e), read length (f).

Supplementary Figure 2



The relation between sequencing depth and the number of high quality genotypes.

- a) We observe a strong relation between the number of sequenced bases and the number of high quality genotypes, we do not observe that paired end sequencing improves genotyping.
- b) We observe that newer samples usually have more bases sequenced.

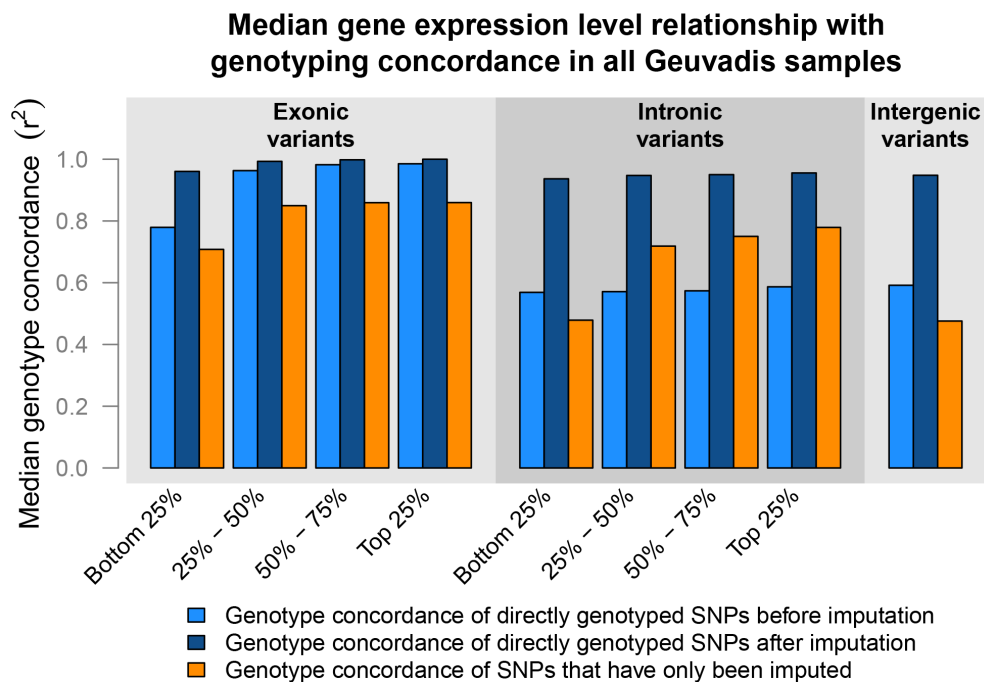
Supplementary Figure 3

Figure provided separately.

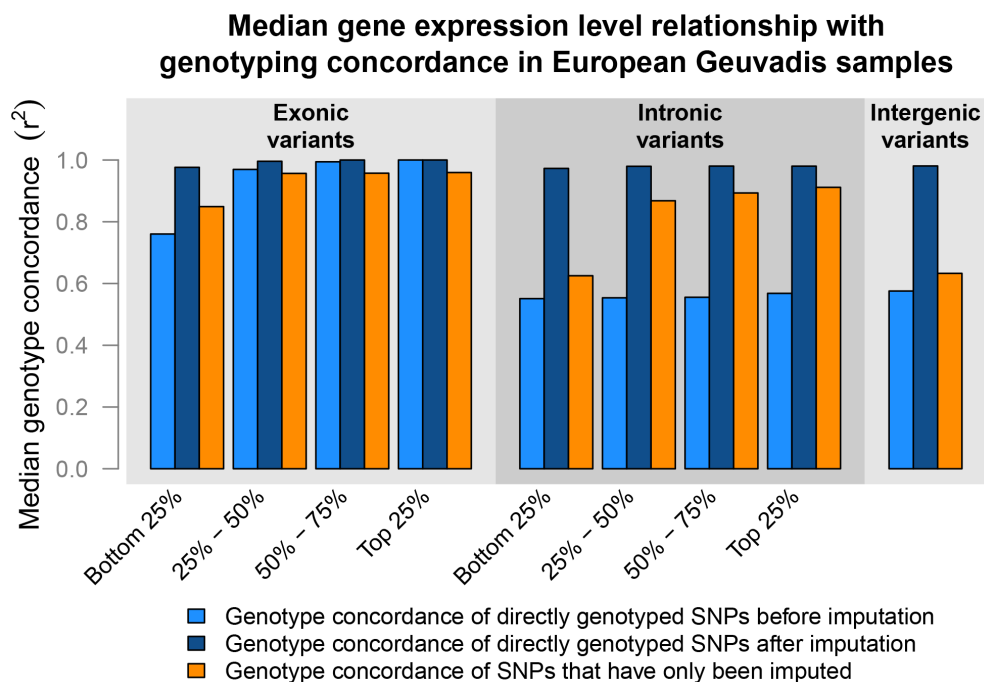
Overview of genotyping accuracy and gene-expression over all chromosomes.

Supplementary Figure 4

a



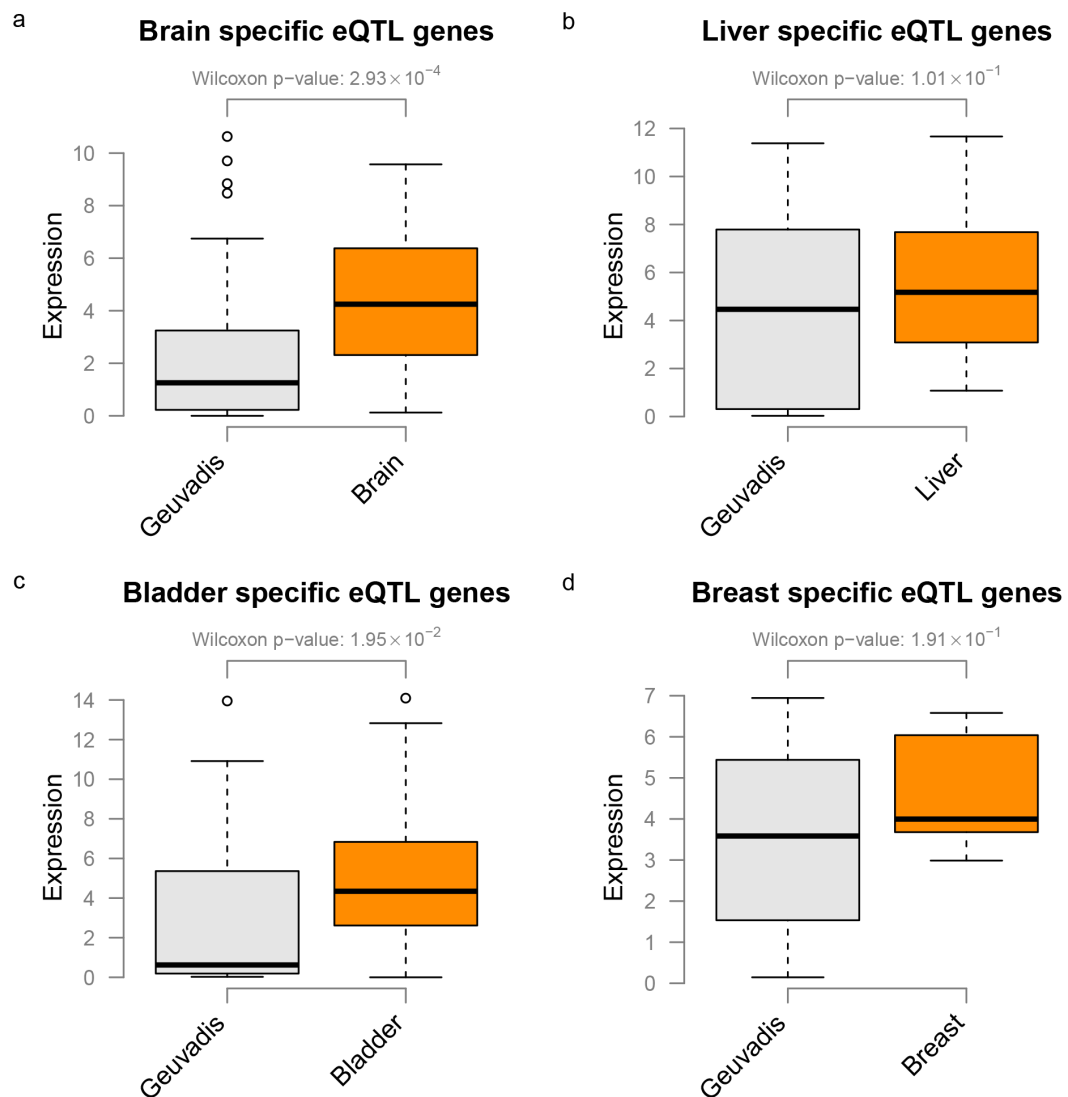
b



Relation between gene-expression levels and genotype concordance before and after imputation.

Genotype concordances in all Geuvadis samples (a) and European Geuvadis samples (b) of common SNPs ($MAF \geq 0.05$, $DR2 \geq 0.8$) before and after imputation grouped by the median expression levels of their genes.

Supplementary Figure 5

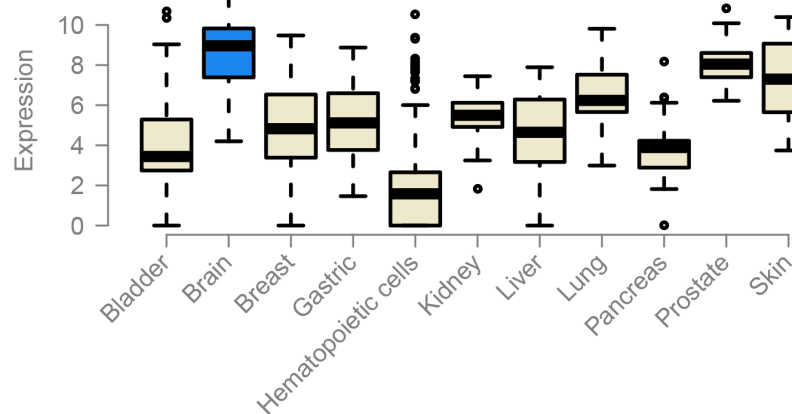


Expression of tissue-specific *cis*-eQTL genes vs Geuvadis expression.

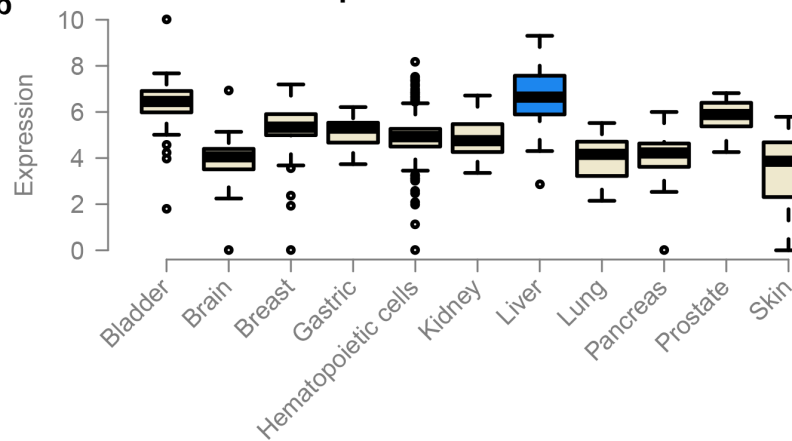
We find that genes with tissue specific *cis*-eQTLs are more abundantly expressed in the respective tissues compared to the Geuvadis samples in which we did not observe the *cis*-eQTLs.

Supplementary Figure 6

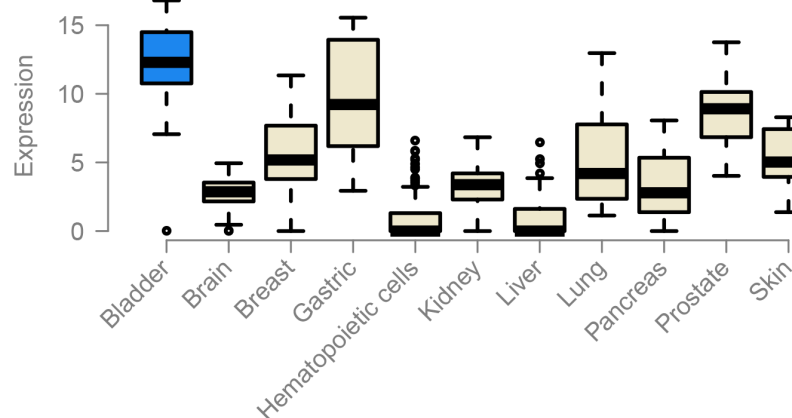
a GSTM5 expression in different tissues



b DDTL expression in different tissues



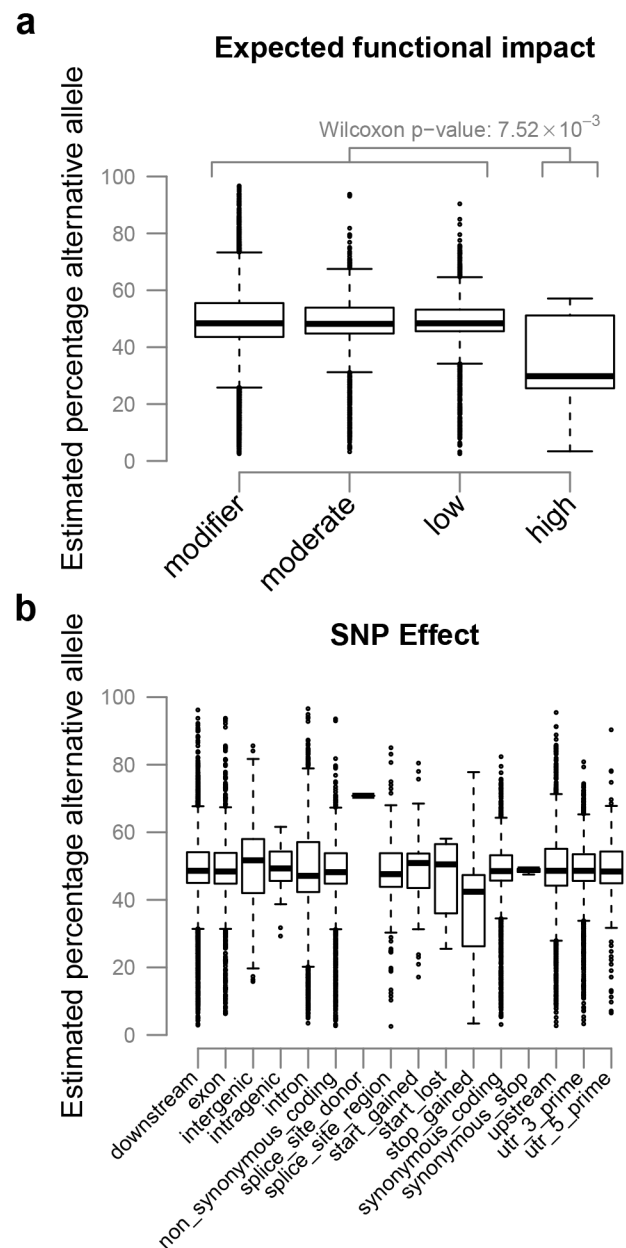
c PSCA expression in different tissues



Expression of example tissue-specific eQTL in different tissues.

Here we show three example tissue-specific eQTL genes: a) *GSTM5*, brain-specific. b) *DDTL*, liver-specific. c) *PSCA*, bladder specific.

Supplementary Figure 7

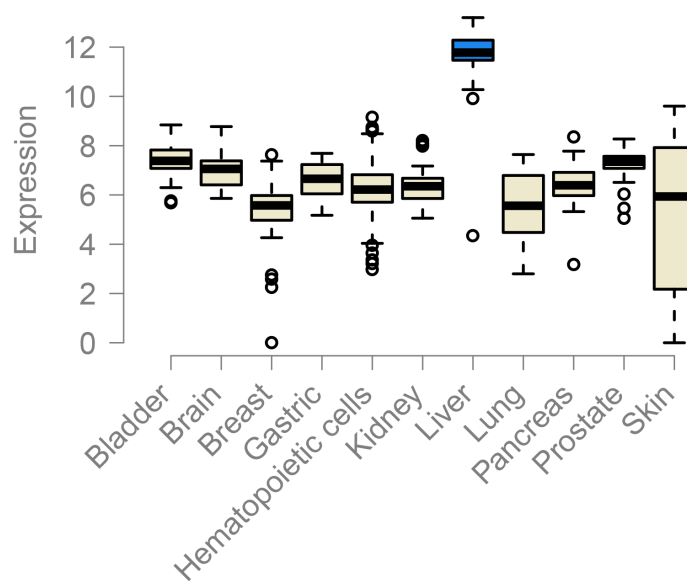


Predicted functional impact of ASE variants.

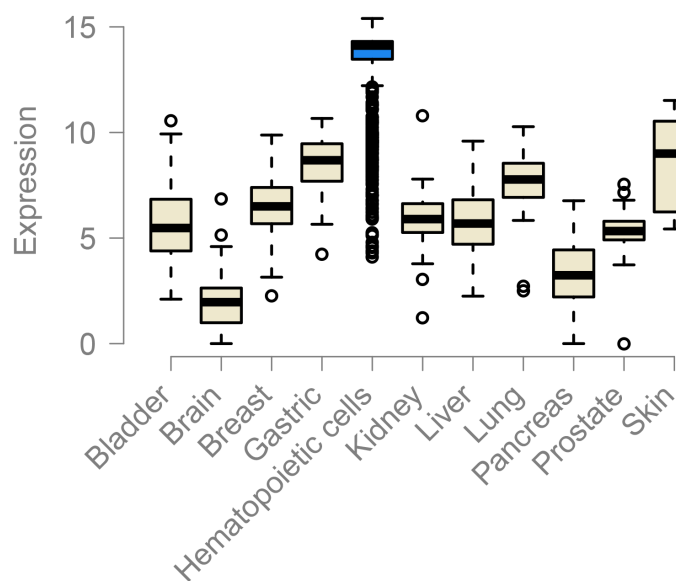
The annotation of ASE SNPs predicted impact and effect was performed using SnpEff. (a) Most of the high-impact SNPs have lower expression of the alternative allele. (b) The majority of the SNPs introducing a stop codon have lower expression of the alternative allele.

Supplementary Figure 8

a MASP2 expression in different tissues



b IRF4 expression in different tissues

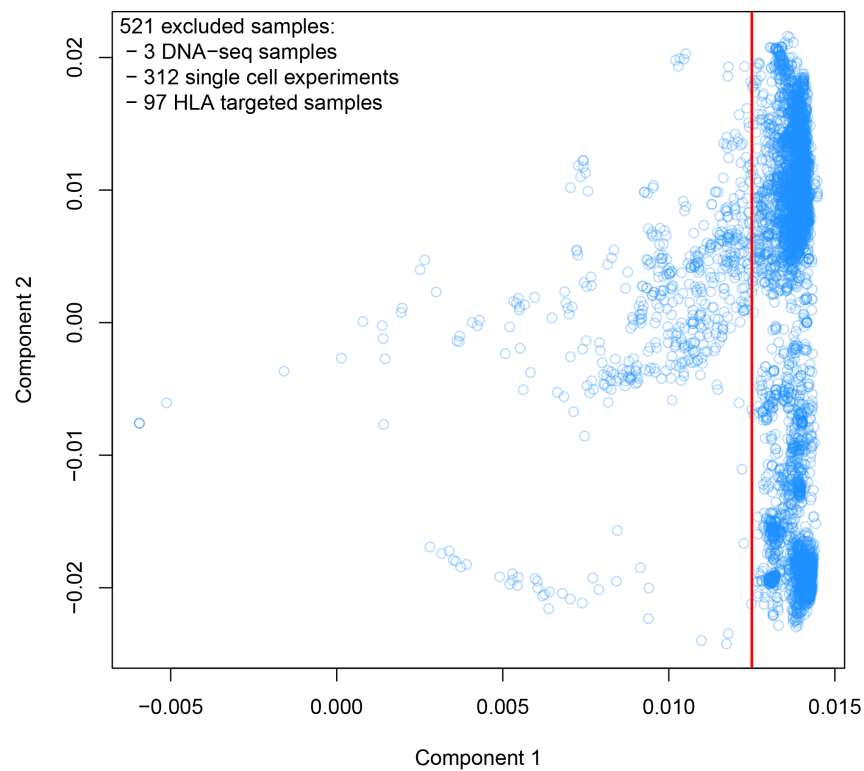


Expression of *MASP2* gene is liver-specific and the expression of *IRF4* gene is hematopoietic-specific.

(a) *MASP2* gene has higher expression in liver compared to other tissues. (b) *IRF4* gene has higher expression in hematopoietic cells compared to other tissues.

Supplementary Figure 9

Sample exclusion using PCA on gene expression levels



PCA on expression values shows strong outliers that are removed from the analysis.

The 521 outliers of the first component (left of the red line) were removed from our analyses.

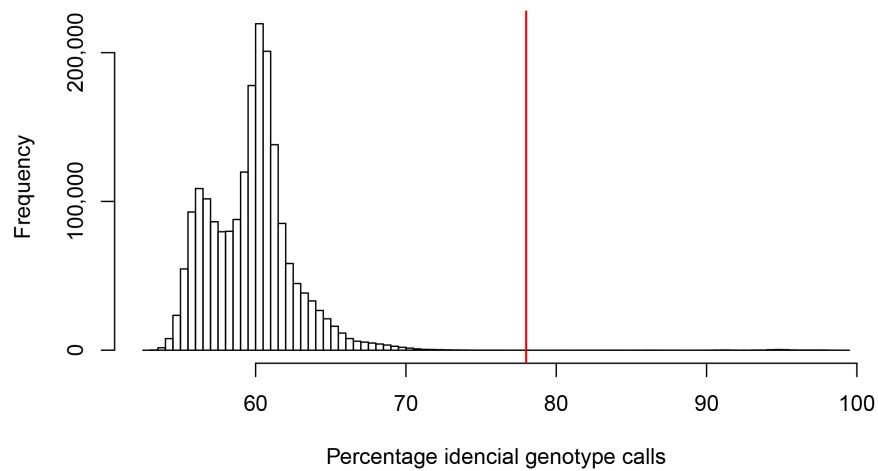
Supplementary figure 10

Figure provided separately.

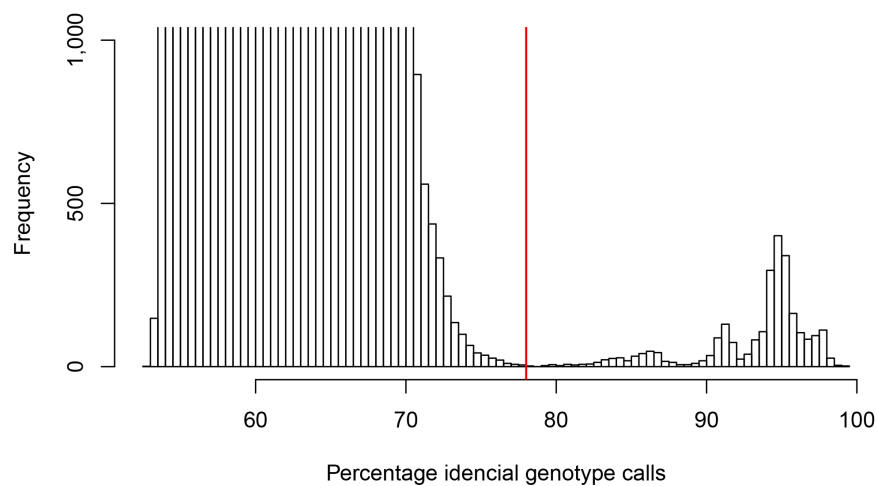
Correlation of principal components vs different confounders.

Supplementary Figure 11

a



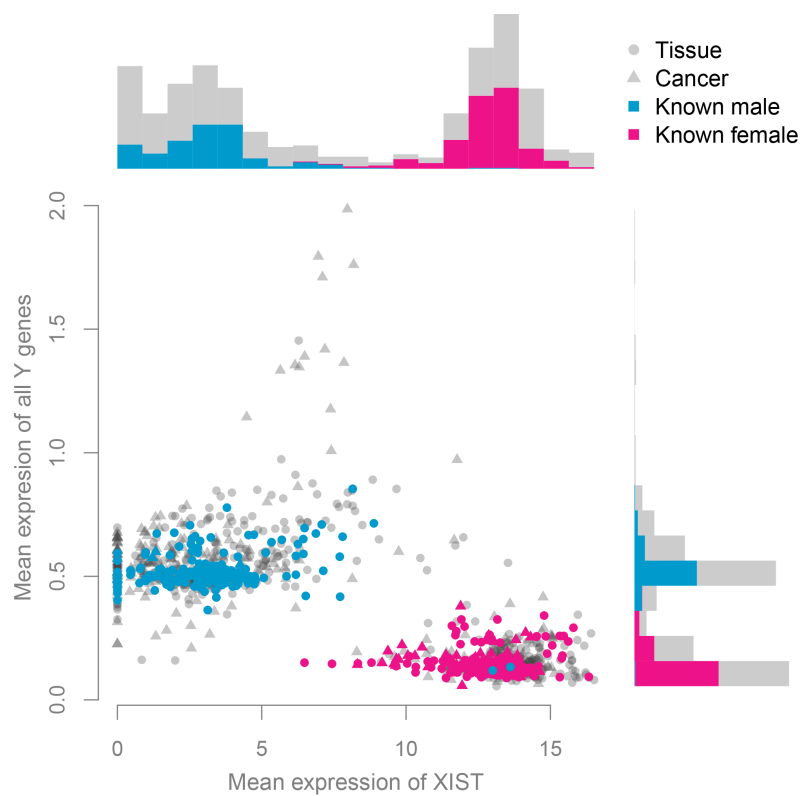
b



Identification of duplicate samples.

We used a cut-off of 78% identity to select duplicate markers. By using this cut-off level we could identify all the duplicates, which we expected based on the annotations. The reason that we have multiple peaks above this cut-off is due to the difference in genotyping quality among the samples. Panel b is the enlargement of the lower part of panel a.

Supplementary Figure 12



Expression of *XIST* and chromosome Y genes.

We show a clear separation of males and females using both *XIST* expression and chromosome Y expression. In two cases, the samples were annotated as male but clustered within the females; these are likely mis-annotations.